

## Chapter 5

# Wave Generation

### 5.1 Wave Generation

When a gentle breeze blows over water, the turbulent eddies in the wind field will periodically touch down on the water, causing local disturbances of the water surface. Small ripples will form, but only where the eddies touch down, since the wind speed must be in excess of 0.23 m/s to overcome the surface tension in the water. Theory (Phillips, 1957 and Miles, 1957) shows wind energy is transferred to waves most efficiently when they both travel at the same speed. But the wind speed is normally greater than the wave speed. For this reason, the generated waves will form at an angle to the wind direction so that the component of the wind speed in the direction of wave propagation approaches the wave speed. At first, because the wave speed is very small, the angle between the wind and the wavelets will be large, forming “cats paws” on the water where the puffs of wind strike. Eventually, the generated wave crests will form a more regular pattern of crossing waves, as shown in Fig. 2.4. At any particular location this will yield short-crested, irregular waves. Even for large waves, when we step back far enough (for example, when we fly high above an ocean) crossing wave crests are clearly identifiable.

Once the initial wavelets have been formed and the wind continues to blow, energy is transferred from the wind to the waves mainly by two mechanisms. A simplistic picture is given in Fig. 5.1. Sheltering causes

the wind speed downwind of the wave to be smaller or sometimes the reverse of the wind speed on the upwind side. The resulting shear on the water surface will tend to move water toward the wave crests from both sides. The form of the wave also causes the wind velocity to increase over the crest and to decrease in the trough. According to Bernoulli's principle, this means the pressure is lower over the crest and higher in the trough. Relative to the mean pressure, the effective pressure over the crest is negative and in the trough it is positive, which will tend to lift the crest and push the trough further down. Thus both the wind shear and pressure differences tend to increase wave height.

Most of the wind energy is transferred to high frequency waves. Thus, the wind causes small waves to form on top of existing waves, rather than increasing the size of the larger waves directly by shear and pressure differences. This pool of high frequency wave energy is then transferred to lower frequencies by the interaction of the high frequency movement with the adjacent slower moving water particles. The process is similar to locally generated sea becoming swell as discussed in Ch. 3.

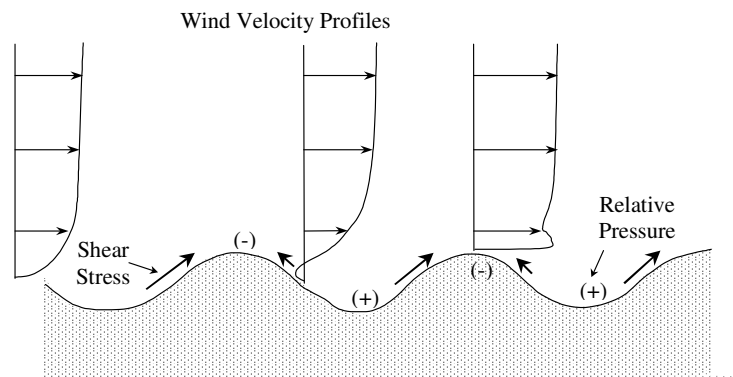


Fig. 5.1 Wind energy transfer

Chapter 2 shows that wave height and period are closely related to wind speed. It should therefore be possible to estimate wave conditions from known wind conditions. In fact, it should be possible to reconstruct a wave climate at a site from historical, measured wind records. Such a computation is known as *wave hindcasting*. *Wave forecasting* is also possible by using forecast wind conditions. Since the procedures are identical we will cover both by the term wave hindcasting.

## 5.2 Simple Wave Hindcasting

### 5.2.1 Introduction to Parametric Methods

The art of defining waves from wind fields came into prominence during World War II. When the Allied forces wanted to land troops on the beaches of Continental Europe, it was critical that weather forecasts could be translated into expected wave conditions. The result of this international war effort was written up by the scientists involved (Sverdrup and Munk, 1947). The method was later extended by Bretschneider (e.g., Bretschneider, 1958) to form the empirical method, now known as the SMB Method. The method is described fully in USACE (1977) and in earlier versions of that publication. In USACE (1984) this method was replaced by the Jonswap Method, based on research on wave spectra in growing seas by Hasselmann et al (1973).

The Jonswap and SMB methods are called parametric methods because they use wind parameters to produce wave parameters, rather than develop a detailed description of the physics of the processes. Although, these methods produce estimates of wave height and period only, they can be extended to provide estimates of the parametric wave spectra discussed in Sec. 3.7.

Parametric wave hindcasting determines wave height and period ( $H$  and  $T$ ) from fetch ( $F$ ), storm duration ( $t$ ) and depth of water in the generating area ( $d$ ). Fetch is the distance over which the wind blows over

the water to generate the waves. For a lake or a bay, fetch is readily determined as the distance into the wind direction from a point of interest to the opposite shore. For irregular shorelines, USACE (1984) suggests that the distance to shore be averaged over  $12^\circ$  on either side of the mean wind direction. For hindcasts on large lakes or the open ocean, fetch is related to the sizes and tracks of the weather systems. Wave forecasting or hindcasting along an open shore is therefore more difficult. Fetches are large and defined by curvatures of the isobars describing the weather systems (USACE, 1984) and hence difficult to define accurately. Fortunately, the wave parameters are not very sensitive to absolute errors in fetch length for these large fetches. As a limit for storms of normal size, changes in wind direction make it unlikely that fetch would be greater than 500 km.

If  $F$ ,  $t$  and  $d$  are all infinite, the result is a *fully developed sea* (Ch. 2). The waves are fully developed so that any added wind energy is balanced by wave energy dissipation rate resulting from internal friction and turbulence. In that case, the resulting wave conditions are a function of wind speed only, as described by the Beaufort scale in Ch. 2. When  $F$ ,  $t$  or  $d$  are limited, the waves will be smaller.

### 5.2.2 Wind

Wind speed varies with distance above the water and the standard height used in wave hindcasting is 10 m. For wind records taken at a different height above the water, a logarithmic velocity profile is assumed so that

$$\frac{U_{10}}{U_z} = \left( \frac{10}{z} \right)^{1/7} \quad (5.1)$$

where  $z$  is the anemometer height. Wind speed is normally quoted as hourly average wind speed. Such hourly wind speeds can be introduced into an hourly wave hindcast (a hindcast that produces wave heights at

hourly intervals as discussed in Sec. 5.3.1). To estimate the wave condition that has built up over a duration  $t$  (without calculating and summing the hourly waves from hourly wind speeds), the concept of effective wind speed is used. One such relationship may be found in USACE (1984). For durations less than 10 hours

$$\frac{U_t}{U_1} = 1 - 0.15 \log t \quad (5.2)$$

where  $U_t$  is the effective wind speed over time  $t$  and  $U_1$  is the maximum of the hourly average wind speeds over time  $t$ .

The wind speed in a wave hindcast computation must be wind speed over the water. Normally we only know wind speeds from nearby airports, and we must take into account that winds over water are usually greater than winds over land, because of the smaller friction over the water. Resio and Vincent (1977) and USACE (1984) provide some coefficients (Fig. 5.2). It is seen that the difference between the wind over the water ( $U_w$ ) and the wind speed over land ( $U_L$ ) is greatest for small wind velocities. Figure 5.2 also proposes a correction factor for the air-sea temperature differences. USACE (1984) introduces an adjustment, based on the wind stress over the water surface, but comparisons of hindcast and measured waves generally show that the use of this correction is not recommended.

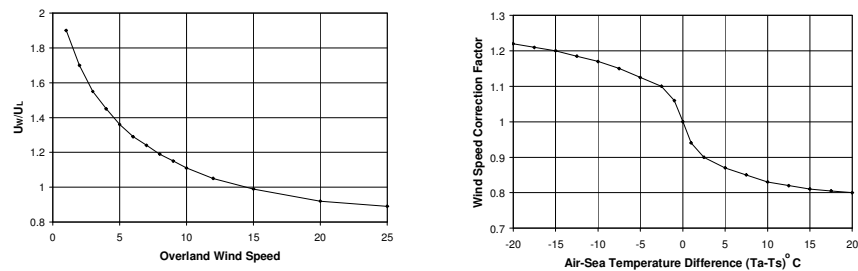


Fig. 5.2 Wind speed corrections (after Resio and Vincent, 1977)

Wind direction can also be quite different over the water than over land (just ask any sailor). An airport wind direction could be up to 30° different from wind direction over water and again this effect is greatest for smaller wind velocities. Since wave direction is usually assumed to be the same as the wind direction, this assumption can be a source of substantial errors in wave direction, which in turn causes large errors in derived quantities, such as alongshore sediment transport rate (Ch. 12). Donelan (1980) and Donelan et al (1985) further show that the largest waves do not come from the wind direction, but from a combination of wind direction and the direction of the longest fetch. On the Great Lakes, therefore, the wave direction is always biased toward the long axis of the lake. Even more pronounced is the wind funneling that takes place along narrow bays, lakes, fjords and rivers. In that case, the wind tends to blow either up or down the bay or river, almost regardless of the wind direction elsewhere. Note that wind and wave directions are defined as the directions from where they come. For example, a wave direction of 90° (from north) means that waves come *from* the east.

### 5.2.3 Jonswap Parameters

The Jonswap method of wave hindcasting uses the following dimensionless expressions.

$$F^* = \frac{gF}{U^2}, \quad H_{mo}^* = \frac{gH_{mo}}{U^2}, \quad T_p^* = \frac{gT_p}{U}, \quad t^* = \frac{gt}{U}, \quad d^* = \frac{gd}{U^2} \quad (5.3)$$

The Jonswap relationships are

$$H_{mo}^* = 0.0016 (F^*)^{1/2} \quad (5.4)$$

$$T_p^* = 0.286 (F^*)^{1/3} \quad (5.5)$$

and

$$t^* = 68.8 (F^*)^{2/3} \quad (5.6)$$

Waves generated in deep water can be fetch limited, duration limited or fully developed sea. On a small body of water, the waves would be limited by a short fetch and  $H_{mo}$  and  $T_p$  can be calculated directly from Eqs. 5.4 and 5.5. On a larger body of water, the same equations apply, but wind duration may limit the size of the waves. Equation 5.6 is then used to calculate an *effective fetch* (the fetch needed to produce the same wave height if the duration had been infinite)

$$F_{eff}^* = \left( \frac{t^*}{68.8} \right)^{3/2} \quad (5.7)$$

When  $F^* < F_{eff}^*$ , the waves are fetch limited and Eqs. 5.4 and 5.5 are used. When  $F_{eff}^* < F^*$ , the waves are duration limited and Eqs. 5.4 and 5.5 are used with  $F_{eff}^*$  substituted for  $F^*$ . Thus the smaller value of  $F^*$  and  $F_{eff}^*$  is used. Finally, a fully developed sea, for a large body of water and a large duration, is calculated using the following upper limits

$$H_{mo}^* = 0.243; \quad T_p^* = 8.13; \quad t^* = 71,500 \quad (5.8)$$

The procedure of computing  $H_{mo}$  and  $T_p$  by Jonswap has been published as a nomogram in USACE (1984), which is shown here in Fig. 5.3. The Jonswap method may be streamlined for computer calculation, as in Fig. 5.4 and the program WAVGEN<sup>®</sup>.

Equations 5.4 and 5.5 show that wave period is closely related to wave height, once fetch length has been defined

$$T_p^* = 20.9 (H_{mo}^*)^{2/3} \quad \text{or} \quad T_p = 9.8 U^{-1/3} H_{mo}^{2/3} \quad (5.9)$$

Thus Eqs. 5.4 and 5.9 could be used instead of Eqs. 5.4 and 5.5.

Because of the large uncertainties in the values of  $U$ ,  $F$  and  $t$  and wave direction, and because the hindcasting relationships themselves are uncertain, all hindcasting results must always be regarded as approximate. It is essential that wave hindcasts are calibrated against observed values. This is discussed further in Sec. 5.4.

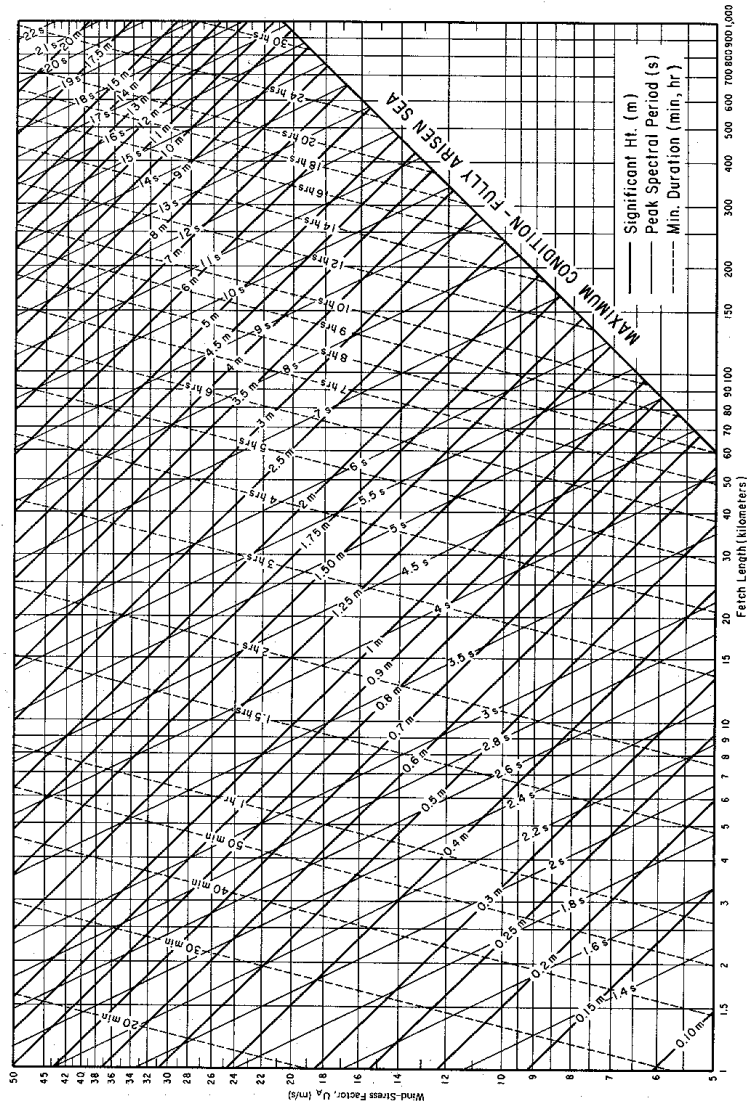


Fig. 5.3 Wave hindcasting nomogram (after USACE, 1984)

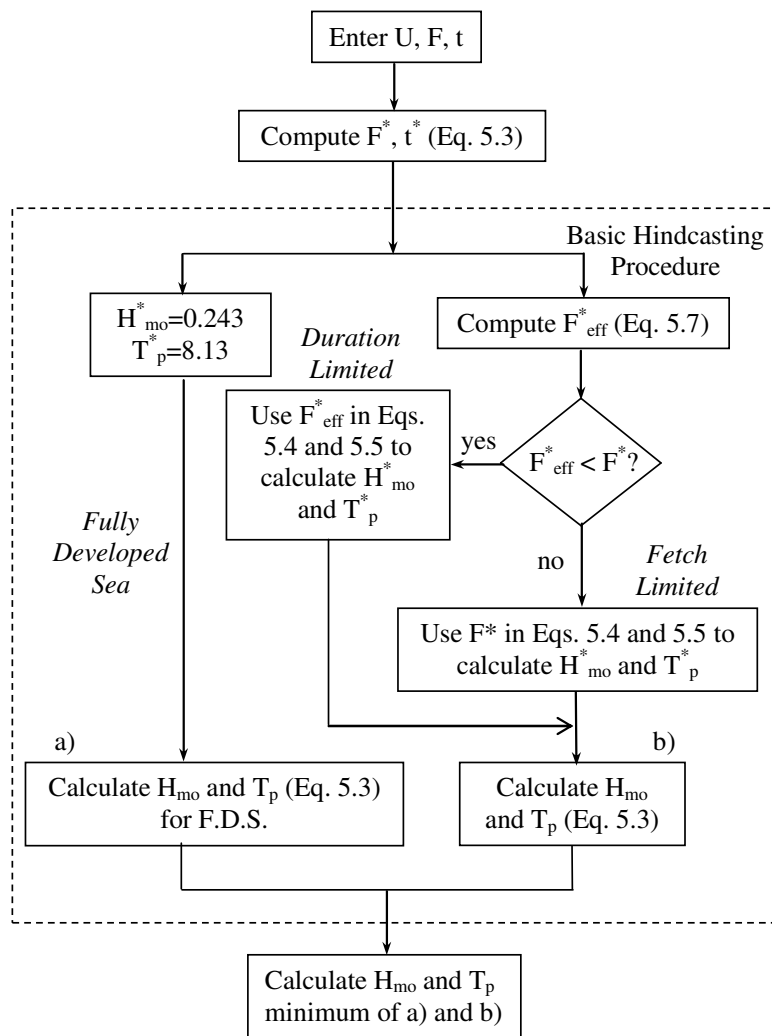


Fig. 5.4 Basic Jonswap hindcasting

---

### Example 5.1 Simple Jonswap wave hindcast

Let us use the Jonswap method to calculate the wave conditions resulting from an effective wind speed  $U = 20$  m/s blowing for 6 hrs ( $t = 21,600$  sec) over a fetch of 100 km ( $F = 100,000$  m). According to Eq. 5.3,  $F^* = 2451.5$  and Eqs. 5.4 and 5.5 yield the fetch limited values  $H_{mo}^* = 0.079$  and  $T_p^* = 3.86$  which in turn (using Eq. 5.3) produce  $H_{mo} = 3.2$  m and  $T_p = 7.9$  sec. These numbers may be confirmed from Fig. 5.3 at the intersection of  $U = 20$  m/s and  $F = 100$  km. Equation 5.7 yields  $F_{eff}^* = 1909$  (or  $F_{eff} = 77.9 \cdot 10^3$  m). Since  $F_{eff}^* < F^*$  the waves are duration limited. Substituting  $F_{eff}^*$  into Eqs. 5.4 and 5.5 yields  $H_{mo}^* = 0.070$ ,  $T_p^* = 3.55$ , and Eq. 5.3 gives  $H_{mo} = 2.9$  m and  $T_p = 7.2$  sec. These results may also be found with Fig. 5.3 at the intersection of  $U = 20$  m/s and  $t = 6$  hrs, which occurs at  $F = 78$  km. A quick check is required to see if the condition for a fully developed sea is exceeded. Comparison of the calculated values with Eq. 5.8 shows that both  $H_{mo}^*$  and  $T_p^*$  are considerably less than the upper limits for a fully developed sea, hence the correct answer is for the fetch-limited condition:  $H_{mo} = 2.9$  m and  $T_p = 7.2$  sec.

---

#### 5.2.4 Maximum Wave Conditions

For many designs and feasibility studies, it is important to identify maximum wave conditions. The above method can yield an estimate of maximum wave conditions, if effective wind speed (Eq. 5.2) is used several times for different values of  $t$ . But it is better to combine known storm segments or actual hourly wind speeds for the growing portion of the storm. To do this, the computation of Fig. 5.4 is repeated for each storm segment (or each hour), as illustrated in Fig. 5.5.

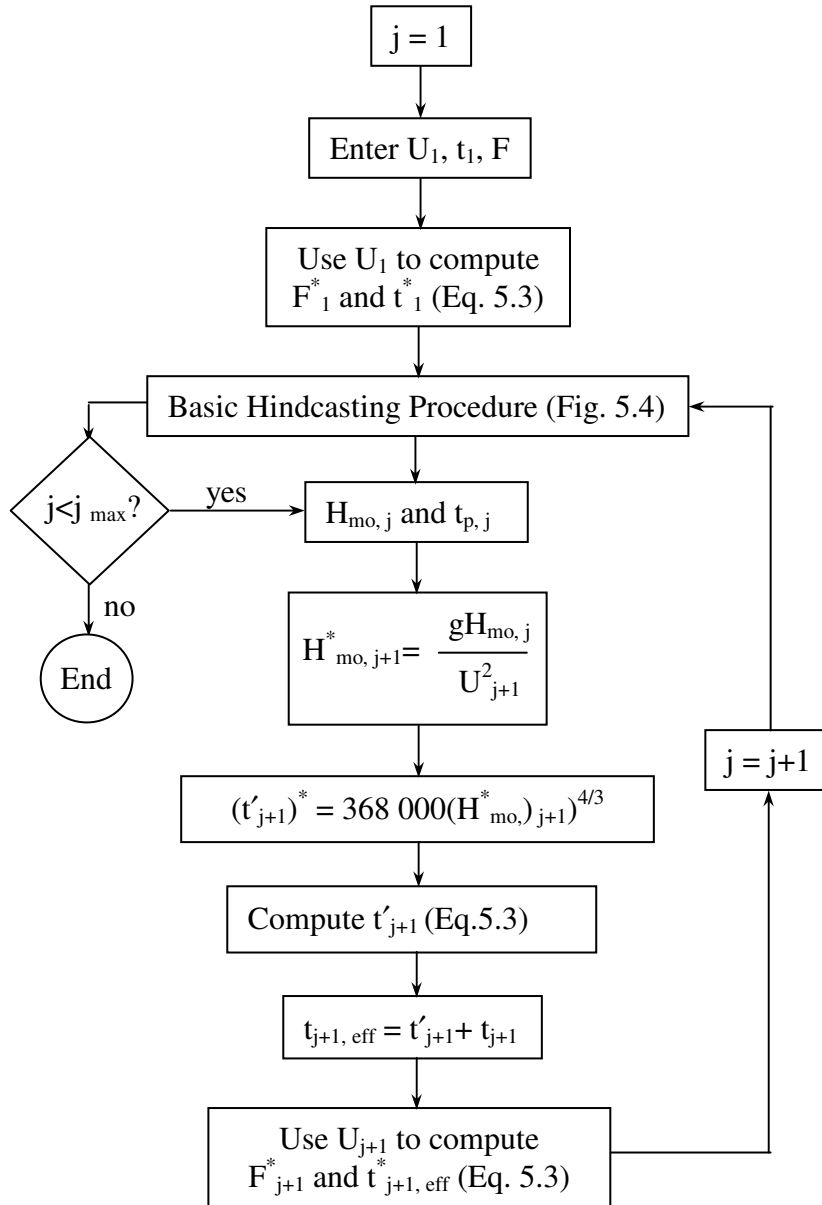


Fig. 5.5 Jonswap hindcasting for a series of input conditions

For the first storm segment, use  $F_1$  and  $t_1$  (where the subscript refers to the first time segment) to determine  $(H_{mo})_1$  and  $(T_p)_1$  at the end of this first segment. The next storm segment will add to the wave energy generated during this first storm segment. Since wave energy is closely related to wave height, we first calculate a virtual storm duration — how long it would have taken for  $(H_{mo})_1$  to be generated by the wind speed of the second storm segment  $U_2$ . We will call this  $(t_2)'$ . To do that, we compute  $(H_{mo,2})^*$  using  $H_{mo,1}$  and  $U_2$

$$H_{mo,2}^* = \frac{g H_{mo,1}}{U_2^2} \quad (5.10)$$

Then Eqs. 5.4 and 5.6 are combined to yield

$$(t_2')^* = 368,000 (H_{mo,2}^*)^{4/3} \quad (5.11)$$

From this,  $t_2'$  may be computed, using Eq. 5.3. We then add  $t_2'$  and  $t_2$  to derive an effective duration  $t_{2,eff}$  of the first two hours at the second wind speed and from this proceed to calculate  $(H_{mo})_2$  and  $(T_p)_2$ . This is repeated for each storm segment until the maximum wave conditions or the maximum number of wind segments is reached. Implicit in such a computation is the assumption that wind direction remains constant. The method works well during the growing part of the storm, when generation of wave energy is far greater than wave energy dissipation.

### 5.2.5 Finite Water Depth

If the depth in the generating area is limited, friction with the bottom will result in smaller waves. USACE (1984) discusses wave generation in finite depth developed by Bretschneider (1958) from Bretschneider and Reid (1953). The expressions were further developed by Young and Verhagen (1996):

$$H^* = 0.24 \left\{ \tanh \left[ 0.49(d^*)^{0.75} \right] \tanh \left[ \frac{0.0031(F^*)^{0.57}}{\tanh [0.49(d^*)^{.75}]} \right] \right\}^{0.87} \quad (5.12)$$

$$T^* = 7.54 \left\{ \tanh \left[ 0.33(d^*) \right] \tanh \left[ \frac{.00052(F^*)^{0.73}}{\tanh [0.33(d^*)]} \right] \right\}^{0.37} \quad (5.13)$$

$$t^* = 537(T^*)^{7/3} \quad (5.14)$$

### 5.3 Hindcast Models

For many applications, simplistic hindcast methods are good enough for first estimates especially of maximum conditions. However, at other times, we need a long-term hindcast wave climate, at hindcast intervals of 1, 3 or 6 hours.

#### 5.3.1 Parametric Models

Parametric, long-term wave hindcasting models are based on the concept of Fig. 5.5. They must, however, also account for wave decay and changes in wind direction. To demonstrate how this is done, imagine that we have correctly hindcast the wave climate at the end of a certain hour. The next hour will have its own wind speed and direction. If there is a large change in wind direction ( $> 45^\circ$ ), we assume that the waves continuing in the old wave direction will stop growing and begin to decay. Waves in the new wind direction will begin to grow. The total wave energy (there may be other decaying wave trains from earlier wind direction changes) is combined to yield  $H_{mo}$  for the next hour. The composite wave period  $T_p$  and wave direction may be calculated by weighting the various contributing wave periods and directions according to the wave energy they contribute. If the change in wind direction is small ( $< 45^\circ$ ), we split up the wave energy into a portion that continues in the previous wave direction,  $E(1-\cos\beta)$  and another portion,  $E\cos\beta$  that accompanies the new wind direction. Here  $\beta$  is the difference between

the new wind and the waves. Waves in the old direction begin decay and waves in the new direction begin to grow.

When the wind speed drops or changes direction, the existing wave energy decays, but at what rate? There are no clear recipes. Because of the short hindcast interval, we assume a simple linear decay rate for wave energy, represented by a decay coefficient (the waves lose a certain fraction of their energy every hour). The correct value of such a coefficient can only be obtained by calibration against measured data and repeating the computation for different values of the decay coefficient can test its sensitivity.

An example plot from HIND, a model based on the above assumptions, is given in Fig. 5.6. It shows 25 days of calculated and observed waves at Grand Bend on Lake Huron. The waves were hindcast using the default coefficients for HIND, which are the values in Eqs. 5.3 to 5.11 and a decay coefficient of 0.3. In general, and in spite of a rapidly changing wind field, the hindcast wave heights, periods and angles are quite good. Some details such as storm peaks and decay after the peaks are not correct, indicating the necessity for calibration and further verification.

### **5.3.2 Wave Spectra Models**

The discussion so far has concentrated on hindcasting  $H_{mo}$ ,  $T_p$  and  $\theta$ . These can be related to parametric wave spectra as discussed in Sec. 3.7. For example, we can formulate a hindcast Jonswap spectrum by substituting the hindcast value of  $T_p$  (or  $f_p$ ) into Eq. 3.56 and adjusting the value of  $\alpha$  to produce the correct hindcast value of  $H_{mo}$ . Chapter 3 also shows how the coefficients and the peak frequency of the Pierson Moskowitz (1964), the Jonswap (Hasselmann et al, 1973) and the Mitzuyasu (1980) spectra are all functions of wind speed and that the spectrum is depth limited through spectral saturation, e.g., Bouws et al (1985, 1987).

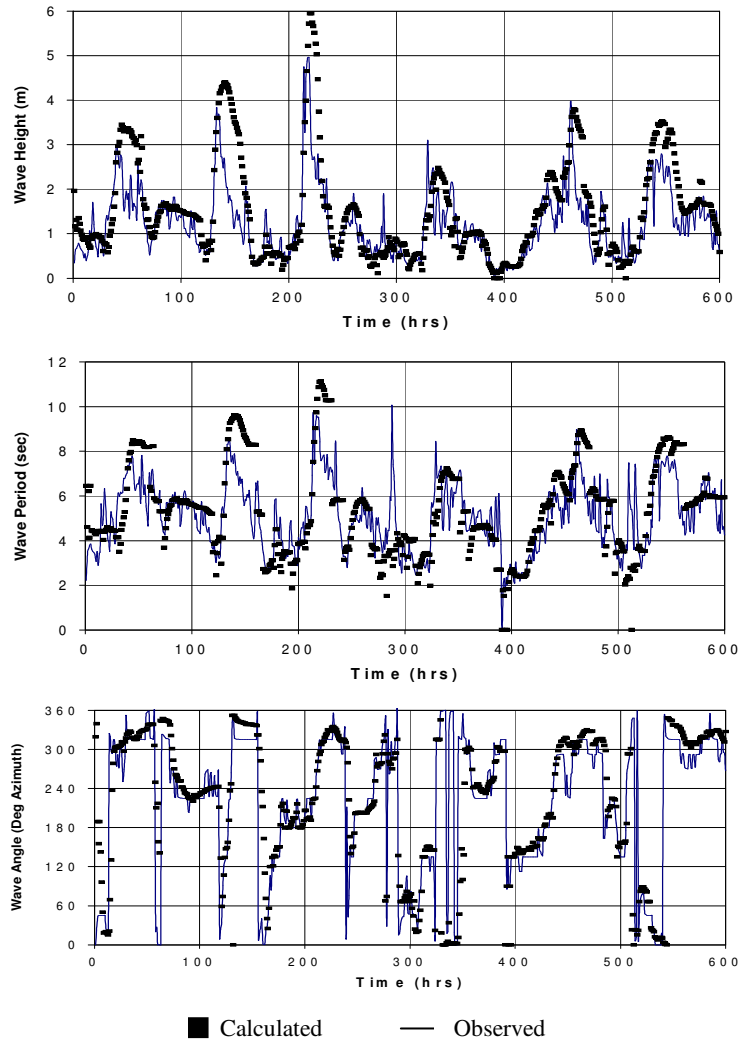


Fig. 5.6 Example hourly wave hindcast

### **5.3.3 More Complex Hindcasting Models**

The above models are all one-dimensional parametric models. More complex models are beyond the scope of this text. They can calculate two dimensional spectral wave fields over large areas. Examples are Schwab et al (1984), Clancy et al (1986), the WAM model (Wamdi, 1988), HISWA (Holthuysen et al, 1989), WAVEWATCH (Tolman, 1991) and SWAN, (Booij et al, 1996, Holthuyjsen, 2006).

## **5.4 Uncertainty**

The basic method of Sec. 5.2 is an approximation, based only on some observations, mainly in the North Atlantic Ocean. There are also no clearly best methods to incorporate changes in wind speed and direction by simple parameters. As a result, all such models must be regarded as very approximate and must be carefully calibrated. The more sophisticated models of Sec. 5.3.3 must be calibrated also. For such calibrated models, Kamphuis (1999) estimates the uncertainties in hindcast waves as  $\sigma'_H = 0.25$ , and  $\sigma'_T = 0.3$ . Burcharth (1992) estimates  $0.1 < \sigma'_H < 0.2$ . The absolute error in hindcast wave direction can be as high as  $30^\circ$  in deep water. In subsequent discussions, we will assume that  $\sigma_{\alpha, \text{Hind}} = 8^\circ$ , which results in  $\sigma'_{\alpha, \text{Hind}} = 0.8$  for a  $10^\circ$  wave angle and causes very large uncertainty in wave direction in shallow water.